Studies of a Hybrid and Multiscale Tumor Growth Model using Isogeometric Analysis

Paulo Wander Barbosa

paulo.w.barbosa@ufes.br

High Performance Computing Lab - Federal University of Espírito Santo

Vitória, Brazil

Adriano M. de Almeida Côrtes

adriano@nacad.ufrj.br

Campus Duque de Caxias *and* High Performance Computing Center - Federal University of Rio de Janeiro

Rio de Janeiro, Brazil

Lucia Catabriga

luciac@inf.ufes.br

High Performance Computing Lab - Federal University of Espírito Santo

Vitória, Brazil

Abstract.

In this work we present experiments in two and three dimensions of a hybrid and multiscale model for tumor growth. The model used can describe tumor growth in the vascular and avascular phase. Two phase field equations and two reaction-diffusion equations form the continuous system of PDEs that is acoupled with an agent-based model. The fields describe tumor tissue and capillaries and the other equations describe nutrients and angiogenic factors. We use the high-performance framework PetIGA based on Isogeometric analysis to implement the model. Our numerical experiments show that the model corresponded well to the introduction of a tensor that mimics the extracellular matrix. It also shows great potential to represent the growth of a tumor cord.

Keywords: *Tumor growth, Angiogenesis, Phase-field models, Mathematical and computational modeling*

1 INTRODUCTION

The cells of our body have genetically programmed mechanisms that control how often they can divide, their differentiation and when their life cycle ends, keeping the appropriate number of each cell type. Genetic and epigenetic changes over time can provoke a lack of control of these mechanisms, creating an agglomeration of cells and thus forming the tumor. Solid tumors account for more than 85% of cancer mortality (Jain, 2005) where carcinoma, solid tumors that develop by the unregulated multiplication of epithelial cells, accounts for most of these deaths. Epithelial cells feed through the diffusion of nutrients found in adjacent connective tissue, named the stroma, that is interlaced by blood vessels, nerves, and lymphatic vessels. Every process involving the origin and development of the tumor is quite complex and involves a large amount of events at different scales: molecular scale, cellular and tissue.

In the early stage, called avascular stage, the tumor cells feed on nutrients that are available in the host tissue and that have penetrated of the tumor surface, and the volume of a tumor, generally, does not exceed 1mm^3 (Koumoutsakos et al., 2013). The growth of a spherical cluster of tumor cells prevents the nutrients from reaching the nucleus by diffusion, forming three regions: proliferative layer, hypoxic layer and necrotic nucleus. The proliferative layer is located in the most superficial part of the tumor and is in contact with the host tissue, therefore it has easier access to the available nutrients. The hypoxic layer is an intermediate layer and the cells of this layer do not have access to the necessary amount of nutrients to proliferate, entering a state quiescent. The necrotic nucleus is formed by cells that for the lack of nutrients necrosed.

The vascular stage will only be reached if the tumor is able to trigger angiogenesis, according to Hanahan & Weinberg (2011), one of the hallmarks of cancer. Angiogenesis is the process of vascularization of a tissue involving the development of new capillary blood vessels from pre-existing blood vessels (Singh, 2004). The regulation of tumor angiogenesis depends on a net balance of angiogenic factors and antiangiogenic factors, which are secreted by both tumor cells and host-infiltrating cells (Pang & Poon, 2006). In normal situations the body has angiogenic factors and antiangiogenic factors in equilibrium. When tumor cells are deprived of nutrients and become hypoxic, they release angiogenic factors that disturb this balance, making angiogenic factors prevail.

The angiogenic factors diffuse through the tumor and host tissue in search of nutrient-rich blood vessels. The blood vessels are lined with endothelial cells that upon contact with angiogenic factors elicit two different phenotypes: stalk and tip. Endothelial cells with the tip phenotype are able to analyze the surrounding environment and move in the correct direction of the tumor, guided by the angiogenic factor gradient. Endothelial cells with the stalk phenotype proliferate creating a new capillary, maintaining the connection between the tip cell and the original vessel. Figure 1 shows a scheme of the growth of a new capillary from a pre-existing vessel. Vascularization provides nutrients necessary for proliferation of tumor cells and an opportunity for migration to other organs through the bloodstream.

A mathematical model describing each of the numerous events taking place in the three scales and the interplay between them is challenging. Even though limited to carcinomas, the model considered in this work (Xu et al., 2016) is multiscale in nature, particularly in the interplay between the tissue and cell scales within the angiogenesis process, marking the transition from the avascular to the vascular phases. Because of this transition we call it also a hybrid model of tumor growth. A very good literature review is found in Cristini & Lowengrub (2010).

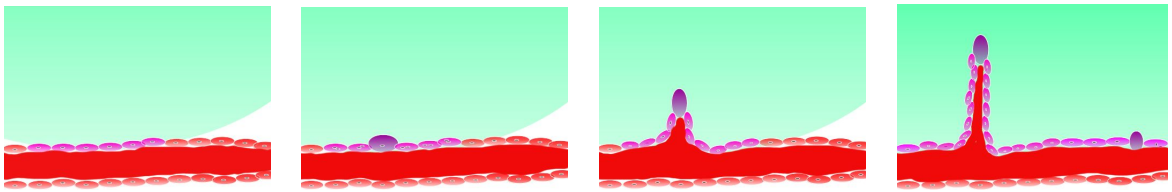

(a) The angiogenic factor concentration (green) reaches the endothelial cells.

(b) One of the endothelial cells assumes the tip phenotype and the other stalk.

(c) The tip cell moves toward the tumor and the stalk cells proliferate.

(d) The angiogenic factor reaches other endothelial cells and another tip cell is activated.

Figure 1: Growth of new capillaries from pre-existing vessels.

In this work we discuss experiments in two and three dimensions of a hybrid and multiscale model of tumor growth (Xu et al., 2016), which is based on a system of partial differential equations coupled with an agent-based model requiring extensive computational resources. To satisfy such requirement, we used a high performance Isogeometric Analysis framework, named PetIGA (Dalcin et al., 2016). The rest of this paper is organized as follow. In Section 2, the mathematical model is presented. Section 3 is dedicated to show the numerical and computational strategies considered to discretize the system of equations describing the model. Section 4 presents the numerical results for a set of experiments. Conclusions and directions for future work are included in Section 5.

2 MATHEMATICAL MODEL

The model is composed of a system of partial differential equations modeling the tumor dynamics, the angiogenesis process, and the tumor angiogenic factor (TAF) and nutrients diffusion, as well as, the interaction between them, hereafter called the continuous part of the model (Xu et al., 2016); coupled with an agent-based model describing the activation, deactivation and migration of endothelial cells with tip phenotype, hereafter called the discrete part (Lima et al., 2014; Vilanova et al., 2013; Travasso et al., 2011).

2.1 Continuous part

The continuous system of PDEs is nonlinear of fourth order and time dependent, where ϕ, c, f and σ the unknowns. The continuous phase field $0 \leq \phi \leq 1$ describes the host tissue ($\phi \approx 0$) and the tumor ($\phi \approx 1$) phases; the phase field $-1 \leq c \leq 1$ describes the avascular tissue ($c \approx -1$) and the capillaries ($c \approx 1$) phases; the field $0 \leq f \leq 1$ determines the balance concentration between pro- and anti-angiogenic substances; and $0 \leq \sigma \leq 1$ determines the concentration of nutrients available. Phase field models have their origin in the material science community, and its application to tumor growth models is discussed in Cristini et al. (2009) and Oden et al. (2010). When $\phi \approx 1$, the amount of nutrients defines three types of cell inside the tumor: proliferative ($\sigma \geq 0.4$), necrotic ($\sigma \leq 0.2$) and hypoxic ($0.2 < \sigma < 0.4$), according to Xu et al. (2016).

The system of differential equations is defined over $\Omega \times (0, T)$, where $\Omega \subset \Re^2$ is a rectangular domain and boundary Γ with an outward unit normal $\mathbf{n}$ and $(0, T)$ is the time interval. The problem can be formulated as

Find ϕ, c, f e σ such that

$$\frac{\partial \phi}{\partial t} = M_\phi(\lambda_\phi^2 \Delta\phi - \mu_\phi(\phi, \sigma)) \tag{1}$$

$$\frac{\partial c}{\partial t} = \nabla \cdot (M_c \nabla(\mu_c(c) - \lambda_c^2 \Delta c)) + \mathcal{B}_p(f) c \mathcal{H}(c) \tag{2}$$

$$\frac{\partial f}{\partial t} = \nabla \cdot (D_f \nabla f) + \phi(1-f)\mathcal{G}(\sigma) - B_u f c \mathcal{H}(c) \tag{3}$$

$$\frac{\partial \sigma}{\partial t} = \nabla \cdot (D_\sigma \nabla \sigma) + V_p^c (1-\sigma) c \mathcal{H}(c) \mathcal{S} - V_u^T \sigma \phi - V_u^H \sigma \mathcal{H}(1-\phi) \tag{4}$$

considering a set of known initial and boundary conditions in $\Gamma \times (0, T)$ such as:

$$\nabla\phi \cdot \mathbf{n} = 0 \quad \nabla(\mu_c(c) - \lambda_c^2 \Delta c) \cdot \mathbf{n} = 0$$
$$\Delta c = 0 \quad \nabla f \cdot \mathbf{n} = 0 \quad \nabla\sigma \cdot \mathbf{n} = 0$$

where M_ϕ represents the tumor mobility and M_c is the mobility for the endothelial cells. D_f and D_σ represent the diffusion coefficients of f and σ, respectively. The parameter λ_ϕ is a length scale that defines the thickness of the diffuse interface between the tumor and the host tissue, and λ_c is a length scale that defines the thickness of the capillary wall. The functions μ_ϕ and μ_c are the tumor and the capillary chemical potentials Cristini et al. (2009); Oden et al. (2010) respectively, given by

$$\mu_\phi(\phi, \sigma) = 2\phi(1-\phi)(1-2\phi) - \frac{12}{3.01\pi}\phi(1-\phi)\arctan(15(\sigma - \sigma^{h-v})) \tag{5}$$

$$\mu_c(c) = c^3 - c \tag{6}$$

The proliferation rate of the endothelial cells is given by the function $\mathcal{B}_p(f)$ and the proliferation rate of the f is given by the constant B_u. Function $\mathcal{G}$ is the secretion rate of tumor angiogenic factor released by tumor cells. Function $\mathcal{S}$ is a crude measure of the structure and density of the capillary network, and for numerical reasons, $\mathcal{H}$ is a smoothed-out Heaviside step function. The constant values V_p^c, V_u^T and V_u^H represent, respectively, the production rate of nutrient, uptake rate of nutrient by tumor and uptake rate of nutrient by host tissue.

2.2 Discrete part

The discrete part controls, between a time step and another, the activation and advancement of the tip cell. Travasso et al. (2011) consider the advance of the tip cell according to a vector $\mathbf{v}$, which is a multiple of the gradient function that describes the angiogenic factor. To describe the resistance of the movement in some directions Lima et al. (2014) used the same vector $\mathbf{v}$ multiplied by a random tensor $\mathbf{k}$. Xu et al. (2016) incorporated into the cell's movement a change in the speed of advancement upon contact with the tumor. The ideas considered by Lima et al. (2014) provided a more realistic shape to the created capillaries, whereas the Xu et al. (2016) considerations prevented the new capillary from crossing the tumor at the same velocity as it had in the extracellular matrix. In this work we consider the continuous part of the mathematical model as described in Xu et al. (2016) and both ideas considered by Xu et al. (2016) and Lima et al. (2014) for assembly the tip cell velocity vector in the discrete part of the model. We set the activation of the part only every 4 time steps.

When the discrete part is triggered, points in a very fine subgrid of the discretized domain, occupied by an endothelial cell, is evaluated for the conditions for a phenotypic change to

migratory phenotype, that is, to become a tip endothelial cell. The conditions are: (*i*) the point is inside a capillary; (*ii*) the nearby concentration of TAF is above a threshold level; and (*iii*) the distance to any other active tip endothelial cell is larger than δ_4, the effective Delta-like ligand 4 distance. These conditions, coupling the continuous and the discrete parts, are mathematically represented by

$$c(\mathbf{x}) \geq c_{act}, \tag{7}$$

$$f(\mathbf{x}) \geq f_{act}, \tag{8}$$

$$\|\mathbf{x} - \mathbf{x}_{tip}^j\| \geq \delta_4, \quad \forall j = 1, ..., N_{tip}(t_n), \tag{9}$$

where $\mathbf{x}_{tip}^j$ is the center of Ω_{tip}^j, one of the $N_{tip}(t_n)$ active tip endothelial cells at instant t_n. Among the points that satisfy those conditions one of them, namely $\mathbf{x}_{tip}^k$, is randomly chosen to be activated, generating a new tip Ω_{tip}^k domain (cell). A subdomain Ω_{tip}^j will be deactivated if the center $\mathbf{x}_{tip}^j$ does not satisfies any of the conditions (7), (8) or (9). Subdomains created between the time steps must be introduced into the problem in the following time step to calculate the solution. In Xu et al. (2016) the new subdomains, created in the discrete part, were incorporated into the continuous part with the aid of the model functions, smooth representations of the phase changes. In our code was made a projection of the discontinuous function, which has value 1 on the subdomain and c value over other domain points. The projection was very efficient, smoothing and eliminating the discontinuity of the function.

Additionally, the current active tip endothelial cells migrate according to

$$\mathbf{x}_{tip}^j := \mathbf{x}_{tip}^j + \Delta t_n \mathbf{v}_{tip}^j, \tag{10}$$

where $\mathbf{x}_{old} \in \Omega_T^k(t_n)$, $\mathbf{x}_{new} \in \Omega_T^k(t_{n+1})$ and the vector $\mathbf{v}_T^k$ defines the advancing of the tip cell. In this work we consider $\mathbf{v}_T^k$ inspired by definitions of Xu et al. (2016); Sun et al. (2005); Lima et al. (2014) as

$$\mathbf{v}_T^k = \mathbf{K}\left[\chi \frac{\nabla f(\mathbf{x}_T^k)}{\| \nabla f(\mathbf{x}_T^k) \|} \mathcal{I}(\phi)\right] \tag{11}$$

where χ is a chemotactic constant, $\mathcal{I}(\phi) = 0.45[\tanh(50(0.5-\phi))+1.0]+0.1$ is a function that incorporates the observation that capillaries can penetrate into the tumor. The random tensors for two and three dimensions are given by the following expressions:

$$K_{2d} = k_h \begin{bmatrix} v_x^2 & v_x v_y \\ v_x v_y & v_y^2 \end{bmatrix} + \frac{k_h}{k_a} \begin{bmatrix} v_y^2 & -v_x v_y \\ -v_x v_y & v_x^2 \end{bmatrix} \tag{12}$$

$$K_{3d} = k_h \begin{bmatrix} v_x^2 & v_x v_y & v_x v_z \\ v_x v_y & v_y^2 & v_y v_z \\ v_x v_z & v_y v_z & v_z^2 \end{bmatrix} + \frac{k_h}{k_a} \begin{bmatrix} v_y^2 & -v_x v_y & v_y v_z \\ -v_x v_y & v_x^2 & -v_x v_z \\ v_y v_z & -v_x v_z & v_z^2 \end{bmatrix} \tag{13}$$

where $\mathbf{v} = (v_x, v_y)$ in 2d, or $\mathbf{v} = (v_x, v_y, v_z)$ in 3d, is a unitary and random vector, k_h and k_a are a measure of heterogeneity and anisotropy, respectively. Both real numbers are considered here as $k_h = 1$ and $k_a = 5$.

3 COMPUTATIONAL METHOD

The numerical solution of the continuous system (1)-(4) and the discrete part described in Sect. 2 is challenging since the model presents strong non-linearities, besides fourth-order differential operators in space. We used spline-based isogeometric analysis method (IGA) (Hughes et al., 2005) to discretize the system, and implemented it in PetIGA (Dalcin et al., 2016). The software framework PetIGA implements the IGA method on top of PETSc, the Portable, Extensible Toolkit for Scientific Computation (Balay et al., 2016), that is, a library for the solution of scientific problems modeled by partial differential equations.

PetIGA was designed with the philosophy that the user do not need to care with anything else besides the discrete approximation of the system of equations. All the parallelism, that is, domain decomposition, load balance, data communication, and general finite element procedures, like, quadrature, vector and matrix assembly, etc are transparent to the user. The main user's task is to code the Residual vector and the Jacobian matrix of the discrete scheme, in our case a semi-implicit one. With respect to the discrete scheme, the easy generation of quadratic basis functions with continuous derivative within the IGA method context, allowed us to discretize the fourth-order differential operator using a primal formulation, without adding auxiliary variables. Indeed, considering the finite-dimensional space $\mathcal{V}^h \subset \mathcal{V}$ generated by the basis functions $\{N_A\}_{A=1,\dots,n_b}$, where the N_A functions are B-splines of degree 2 and continuity C^1, and defining the discrete fields as

$$
\begin{aligned}
\phi^h(x,t) &= \sum_{A=1}^{n_b} \phi_A(t) N_A(x), \\
c^h(x,t) &= \sum_{A=1}^{n_b} c_A(t) N_A(x), \\
f^h(x,t) &= \sum_{A=1}^{n_b} f_A(t) N_A(x), \\
\sigma^h(x,t) &= \sum_{A=1}^{n_b} \sigma_A(t) N_A(x),
\end{aligned}
$$

we obtain the discrete Galerkin's residual for each field:

$$
\begin{aligned}
R_A^{\phi} &= \left(N_A\ ,\ \dot{\phi}^h\right)_{\Omega} + \left(\nabla N_A\ ,\ M_{\phi}\lambda_{\phi}^2 \nabla \phi^h\right)_{\Omega} + \left(N_A\ ,\ M_{\phi}\mu_{\phi}(\phi^h, \sigma^h)\right)_{\Omega}, \\
R_A^{c} &= \left(N_A\ ,\ \dot{c}^h\right)_{\Omega} + \left(\nabla N_A\ ,\ M_c \nabla \mu_c(c^h)\right)_{\Omega} + \left(\Delta N_A\ ,\ M_c\lambda_c^2 \Delta c^h\right)_{\Omega} - \\
&\quad - \left(N_A\ ,\ \mathcal{B}_p(f^h) c^h \mathcal{H}(c^h)\right)_{\Omega}, \\
R_A^{f} &= \left(N_A\ ,\ \dot{f}^h\right)_{\Omega} + \left(\nabla N_A\ ,\ D_f \nabla f^h\right)_{\Omega} - \left(N_A\ ,\ \phi^h(1-f^h)\mathcal{G}(\sigma^h)\right)_{\Omega} + \\
&\quad + \left(N_A\ , B_u f^h c^h \mathcal{H}(c^h)\right)_{\Omega}, \\
R_A^{\sigma} &= \left(N_A\ ,\ \dot{\sigma}^h\right)_{\Omega} + \left(\nabla N_A\ ,\ D_{\sigma} \nabla \sigma_n^h\right)_{\Omega} - \left(N_A\ ,\ V_p^c (1-\sigma_n^h) c_n^h \mathcal{H}(c_n^h) \mathcal{S}\right)_{\Omega} + \\
&\quad + \left(N_A\ ,\ V_u^T \sigma_n^h \phi_n^h\right)_{\Omega} + \left(N_A\ ,\ V_u^H \sigma_n^h \mathcal{H}(1-\phi_n^h)\right)_{\Omega},
\end{aligned}
$$

where $(\cdot\ ,\ \cdot)_{\Omega}$ is the $L^2(\Omega)$ inner product.

For the time integration of the semi-implicit scheme we used the generalized-α method (Chung & Hulbert, 1993), with adaptive time stepping provided by PETSc, and the Jacobian

being calculated according to the scheme. The agent-based model we implemented in C/C++ using STL data structures coupling it with the discretization of the continuous part. Also with respect to the modeling of the angiogenesis process, a switch was added to the model, activating the tensor $\mathbf{K}$ every n steps of time. With this change the model can form a capillary network more sinuous or more rectilinear, according to the value of n chosen.

4 NUMERICAL EXPERIMENTS

In this section we present two experiments. The two-dimensional experiment verifies the model ability to create a network of capillaries in the direction of the tumor after the switch is activated and the tensor $\mathbf{K}$ begins to work. The three dimensional tests the ability of the model to represent different configurations of tumor growth. In all experiments, the tumor and the necrotic nucleus initially occupy circular and concentric regions, the radius of the necrotic part being equivalent to 45% of the tumor radius. Initially there is a quantity $\sigma = 1.0$ in the capillaries, $\sigma = 0$ in the necrotic nucleus and $\sigma = 0.45$ in the other parts of the domain (Xu et al., 2016). The angiogenic factor has an initial concentration of $f = 0.3$ in the tumor and $f = 0$ in the other points of the domain. The values adopted for the constants for the *in silico* experiment, showed in Table 1, are the same as those used in Xu et al. (2016). We consider a length scale L $= 1.25\mu$m and a time scale T $= 1562.5$s to find the values of the physical parameters from the *in silico* quantities.

Table 1: Simulation Parameters - *in silico* values

Symbol	Parameter	*In silico* values	Unit
M_ϕ	Diffusion coefficient of the tumor	0.3	[T^{-1}]
λ_ϕ	Interface width of tumor	$2\sqrt{2}$	[L]
M_c	Mobility of capillaries	1.0	[L^2T^{-1}]
λ_c	Interface width of capillaries	1.0	[L]
B_u	Uptake rate of f by capillaries	6.25	[T^{-1}]
D_f	Diffusion coefficient of f	100.0	[L^2T^{-1}]
D_σ	Diffusion coefficient of the nutrient	30.0	[L^2T^{-1}]
V_p^c	Production rate of nutrient	1.0	[T^{-1}]
V_u^T	Uptake rate of nutrient by tumor	0.006	[T^{-1}]
V_u^H	Uptake rate of nutrient by host tissue	0.0006	[T^{-1}]

4.1 Two dimensional experiment - Tumor close to two vessels

In this experiment a circular tumor of 200μm radius is placed in the center of a 1000μm side square domain, discretized by a mesh with $256C^1$ quadratic elements in each direction. At the top of the domain there is a straight vessel at a distance of 200μm from the tumor and at the bottom there is another at a distance of 237μm from the tumor, as shown in Fig. 2(a). In

this experiment $\lambda_\phi = 2\sqrt{2}$ and the switch is activated every 12 time steps. Initially the tumor consumes all the nutrients around it, growing rapidly until its radius reaches 210μm. After this time there is a slow and uniform reduction until the radius reaches 201μm, almost returning to its initial size. Meantime, at that moment the first capillary arrives at the tumor, taking nutrients the tumor cells return to proliferate. It was about 9 hours until the angiogenic factor touched the vessel and awakened the first cell tip. In about 2 and a half hours the first capillary reached the tumor. After the arrival of new capillaries, the tumor cells proliferate more rapidly. In Fig. 2(b) we can see capillaries feeding the tumor and new capillaries growing in their direction.

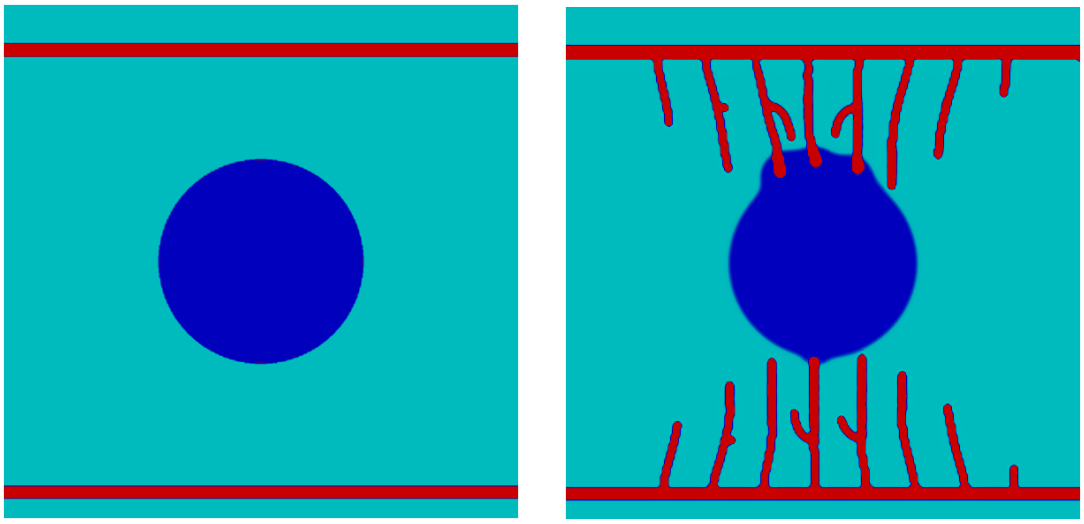

(a) Initial configuration of the vessel and tumor.

(b) Tumor cells proliferate with the arrival of nutrients.

Figure 2: The formation of the new capillary network.

The final behavior of the nutrient and the angiogenic factor are shown in Figs.3(a)-3(b).

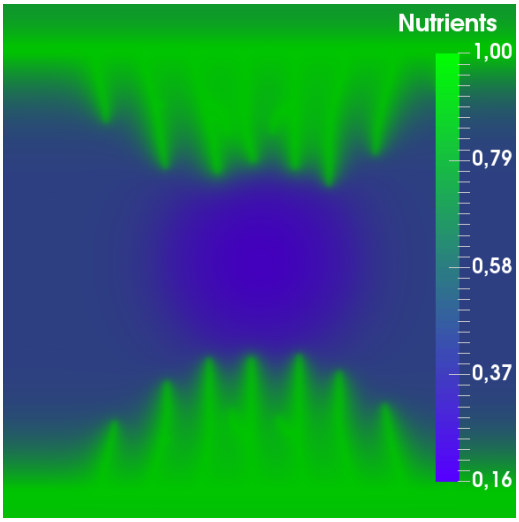

(a) Final configuration of σ.

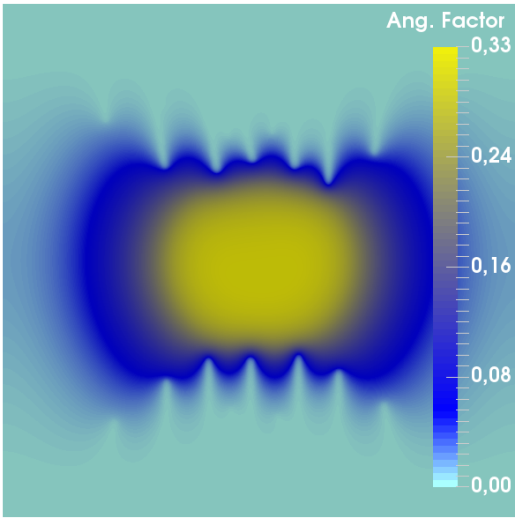

(b) Final configuration of f.

Figure 3: Nutrient and angiogenic factor in the final configuration.

4.2 Three dimensional experiment - Tumor cords

The three dimensional experiments verifies the ability of the model to represent a configuration of tumor growth different from those already tested. In some tumours, the viable cells grow around blood vessels forming cylindrical structures called tumour cords (Bertuzzi et al., 2002). The tumor cord was studied in Moore et al. (1985), Bertuzzi & Gandolfi (2000), Bertuzzi et al. (2004) and Astanin & Preziosi (2009). Models et al. (2008) states that, these cases, the proliferative zone will be (internal) next to the nutrient supply and the necrotic zone will be the outermost layer. In Astanin & Tosin (2007) the simulations show localization of the tumour within a limited distance from the vessels and constant expansion velocity along the vessels. Here, we consider two vessels configurations for the 3D experiments, curve and straight. For both we consider $\lambda_\phi = 8$. The three-dimensional domain measuring 1000μm $\times$ 1000μm $\times$ 750μm is discretized by a mesh with $40C^1$ quadratic elements in each direction.

First, a spherical tumor with 200μm radius is placed in the vicinity of a straight vessel . According to Harris (2002), 180μm is the calculated distance that oxygen diffuses as it passes from the capillary to the cells before it is completely metabolized. In this experiment the distance between the pre-existing vessel and the tumor is of 112μm (see Fig. (4)), thus allowing the arrival of nutrients from the capillary to feed the tumor. The tumor cells proliferated towards the vessel, assuming its shape, as shown in Figs. 4(b)-4(f).

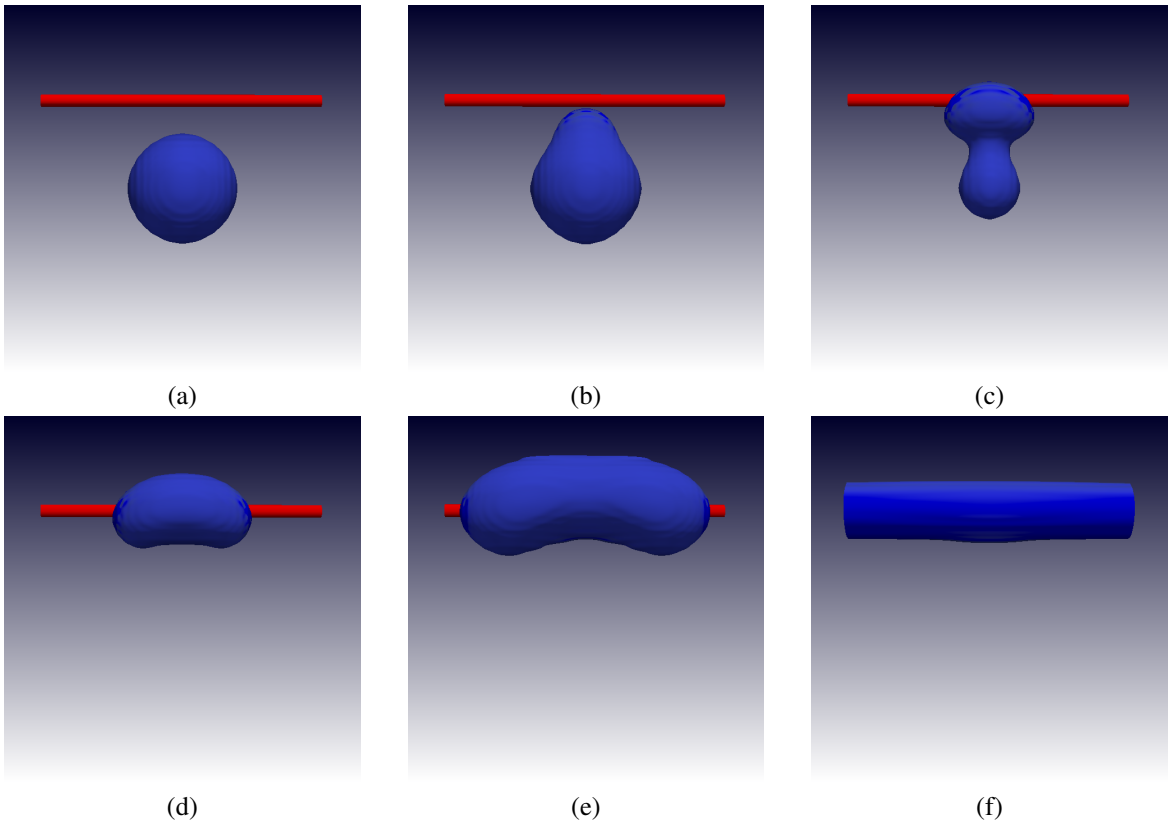

Figure 4: Sequence of proliferation and movement of tumor towards a straight vessel.

The capillary completely surrounds the vessel, as one can see in Figs. 5(a)-(b).

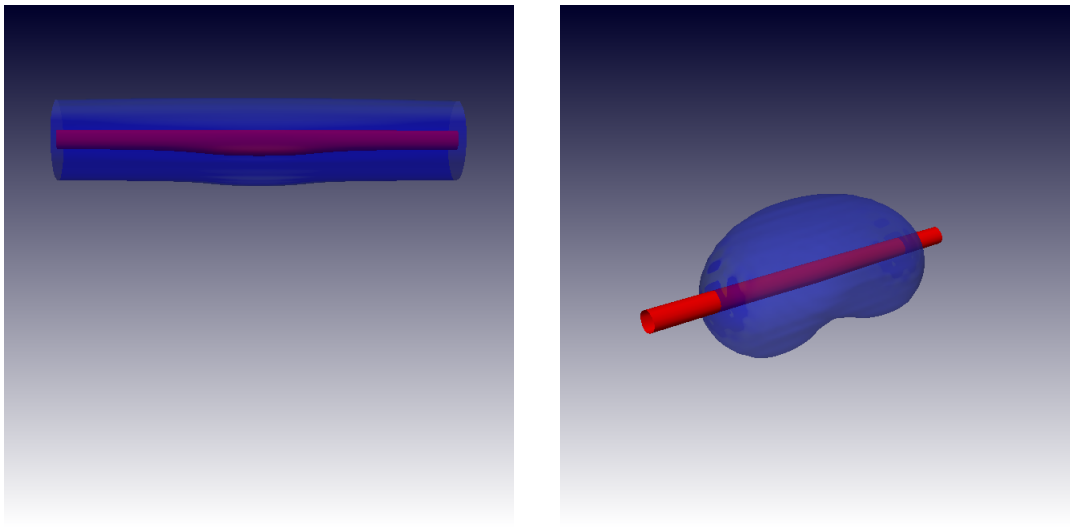

(a) Final configuration of the experiment. (b) Lateral view of one of the stages.

Figure 5: Vision of the vessel in the inner part through the transparency of ϕ.

In the last experiment, we consider a spherical tumor of 175μm radius at a distance of 80μm from a curved vessel, Fig. 6(a). The tumor assumes the shape of the pre-existing vessel, maintaining a constant layer along the vessel, as we can see in Fig. 6. Thus, the model is capable of adjusting to different vessel formats.

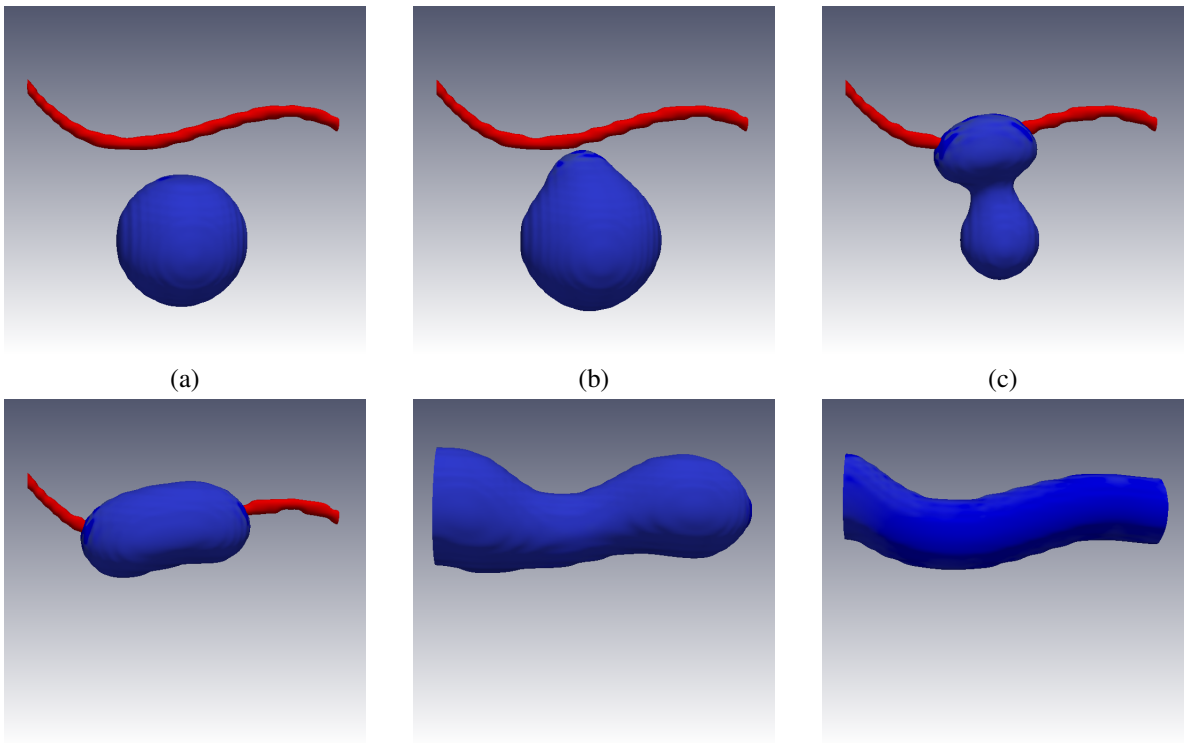

(a) (b) (c)

(d) (e) (f)

Figure 6: Sequence of proliferation and movement of tumor towards the curved vessel.

5 CONCLUSIONS

In this work we present experiments in two and three dimensions related to an implementation of a model hybrid and multiscale tumor growth model, using PetIGA. The model is composed of a system of partial differential equations modeling the tumor dynamics, named continuous part, and an agent-based model describing the activation, deactivation and migration of endothelial cells with tip phenotype, called the discrete part.

Numerical experiments have shown that the model can represent growth and tumor growth in the avascular phase and the recruitment of a capillary network to trigger the vascular phase. The switch added to the model provided the possibility of rapid change in the formation of the capillary network, facilitating subsequent experiments related to the resistance of the extracellular matrix. The model demonstrated great ability to represent the development of the tumor cord.

Our next step includes exploring the high-performance computing provided easily in the PetIGA framework, considering, for example, refined finite element meshes for more accurate simulations. Finally, an important research topic that can be explored is the incorporation of the tip cell movement into the continuous system.

ACKNOWLEDGEMENTS

We would like to thank Dr. E.B.F. Lima from ICES/Texas-UT and Dr. R.C. Almeida from LNCC/MEC-Brazil, by their discussions throughout the course of this work. We also indebted to Dr. L. Dalcin from ECRC/KAUST by his invaluable comments with the implementation of the computational model in the PetIGA framework.

REFERENCES

Astanin, S. & Preziosi, L., 2009. Mathematical modelling of the Warburg effect in tumour cords, *J. Theor. Biol.* 258, 578–590.

Astanin, S. & Tosin, A., 2007. Mathematical model of tumour cord growth along the source of nutrient, *Math. Model. Nat. Phenom.* 2(3), 153–177.

Balay, S., Abhyankar, S., Adams, M. F., Brown, J., Brune, P., Buschelman, K., Dalcin, L., Eijkhout, V., Gropp, W. D., Kaushik, D., Knepley, M. G., McInnes, L. C., Rupp, K., Smith, B. F., Zampini, S., Zhang, H. & Zhang, H., 2016. PETSc users manual, Technical Report ANL-95/11 - Revision 3.7, Argonne National Laboratory.
URL: *http://www.mcs.anl.gov/petsc*

Bertuzzi, A., Fasano, A. & Gandolfi, A., 2004. A free boundary problem with unilateral constraints describing the evolution of a tumour cord under the influence of cell killing agents, *SIAM J. Math. Anal.* 36(3), 882–915.

Bertuzzi, A., Fasano, A., Gandolfi, A. & Marangi, D., 2002. Cell kinetics in tumour cords studied by a model with variable cell cycle length, *Math. Biosci.* 178, 103–125.

Bertuzzi, A. & Gandolfi, A., 2000. Cell Kinetics in a Tumor Cord, *J. Theo. Biol.* 204, 587–599.

Chung, J. & Hulbert, G., 1993. A time integration algorithm for structural dynamics with improved numerical dissipation: the generalized-α method, *J. Apll. Mech.* 60(2), 371–375.

Cristini, V., Li, X., Lowengrub, J. S. & Wise, S. M., 2009. Nonlinear simulations of solid tumor growth using a mixture model: Invasion and branching, *J. Math. Biol.* 58(4-5), 723–763.

Cristini, V. & Lowengrub, J., 2010. *Multiscale Modeling of Cancer: An Integrated Experimental and Mathematical Modeling Approach*.

Dalcin, L., Collier, N., Vignal, P., Côrtes, A. M. A. & Calo, V. M., 2016. PetIGA: A framework for high-performance isogeometric analysis, *Comput. Methods Appl. Mech. Eng.* 308, 151–181.

Hanahan, D. & Weinberg, R. A., 2011. Hallmarks of cancer: The next generation, *Cell* 144(5), 646–674.
URL: *http://dx.doi.org/10.1016/j.cell.2011.02.013*

Harris, A. L., 2002. Hypoxia a Key Regulatory Factor in Tumour Growth, *Nat. Rev. Cancer* 2(1), 38–47.
URL: *http://www.nature.com/doifinder/10.1038/nrc704*

Hughes, T. J. R., Cottrell, J. A. & Bazilevs, Y., 2005. Isogeometric analysis: CAD, finite elements, NURBS, exact geometry and mesh refinement, *Comput. Methods Appl. Mech. Eng.* 194(39), 4135–4195.

Jain, R. K., 2005. Normalization of Tumor Vasculature: An Emerging Concept in Antiangiogenic Therapy, *Science (80-.).* 307(5706), 58–62.
URL: *http://www.sciencemag.org/cgi/doi/10.1126/science.1104819*

Koumoutsakos, P., Pivkin, I. & Milde, F., 2013. The Fluid Mechanics of Cancer and Its Therapy, *Annu. Rev. Fluid Mech.* 45(1), 325–355.
URL: *http://www.annualreviews.org/doi/10.1146/annurev-fluid-120710-101102*

Lima, E. A. B. F., Oden, J. T. & Almeida, R. C., 2014. A hybrid ten-species phase-field model of tumor growth, *Math. Model. Methods Appl. Sci.* 24(13), 2569–2599.
URL: *http://www.worldscientific.com/doi/abs/10.1142/S0218202514500304*

Models, M., Bellomo, N., Li, N. K. & Maini, P. K., 2008. On the foundations of cancer modelling: selected topics, speculations, and perspectives, *Math. Mod. Meth. Appl. Sci.* 18(4), 593–646.

Moore, J. V., Hasleton, P. S. & Buckley, C. H., 1985. Tumour cords in 52 human bronchial and cervical squamous cell carcinomas: Inferences for their cellular kinetics and radiobiology, *Br. J. Cancer* 51, 407–413.

Oden, J. T., Hankins, A. & Prudhomme, S., 2010. General Diffuse-Interface Theories and an Approach To Predictive Tumor Growth Modeling, *Math. Model. Methods Appl. Sci.* 20(03), 477–517.
URL: *http://www.worldscientific.com/doi/abs/10.1142/S0218202510004313*

Pang, R. W. C. & Poon, R. T. P., 2006. Clinical implications of angiogenesis in cancers, *Vasc. Heal. Risk Manag.* 2(2), 97–108.

Singh, Y., 2004. Tumor Angiogenesis: Clinical Implications, *Nepal J. Neurosci.* 1(January 2004), 61–63.

Sun, S., Wheeler, M. F., Obeyesekere, M. & Patrick, C. W., 2005. A deterministic model of growth factor-induced angiogenesis, *Bull. Math. Biol.* 67(2), 313–337.

Travasso, R. D. M., Corvera Poir, E., Castro, M., Rodrguez-Manzaneque, J. C. & Hernndez-Machado, A., 2011. Tumor angiogenesis and vascular patterning: A mathematical model, *PLOS ONE* 6(5), 1–10.
URL: *https://doi.org/10.1371/journal.pone.0019989*

Vilanova, G., Colominas, I. & Gomez, H., 2013. Capillary networks in tumor angiogenesis: From discrete endothelial cells to phase-field averaged descriptions via isogeometric analysis, *Int. j. numer. method. biomed. eng.* 29(1), 1015–1037.

Xu, J., Vilanova, G. & Gomez, H., 2016. A Mathematical Model Coupling Tumor Growth and Angiogenesis, *PLoS One* 11(2), e0149422.
URL: *http://dx.plos.org/10.1371/journal.pone.0149422*